Journal of
Plankton Research

academic.oup.com/plankt

J. Plankton Res. (2022) 1–15. https://doi.org/10.1093/plankt/fbac006

ORIGINAL ARTICLE

Fine-scale vertical distribution and diel migrations of *Pyrosoma atlanticum* in the northern California Current

JOANNA T. LYLE [1,*], ROBERT K. COWEN [2], SU SPONAUGLE [3] AND KELLY R. SUTHERLAND [1]

[1]OREGON INSTITUTE OF MARINE BIOLOGY, UNIVERSITY OF OREGON, 63466 BOAT BASIN RD., CHARLESTON, OR 97420, USA , [2]HATFIELD MARINE SCIENCE CENTER, OREGON STATE UNIVERSITY, 2030 SE MARINE SCIENCE DRIVE, NEWPORT, OR 97365, USA AND [3]DEPARTMENT OF INTEGRATIVE BIOLOGY, OREGON STATE UNIVERSITY, 3029 CORDLEY HALL, CORVALLIS, OR 97331, USA

*CORRESPONDING AUTHOR: jlyle@uoregon.edu

Received July 29, 2021; revised December 9, 2021; accepted January 21, 2022

Corresponding editor: Marja Koski

Blooms of the colonial pelagic tunicate *Pyrosoma atlanticum* in 2014–2018 followed a marine heatwave in the eastern Pacific Ocean. Pyrosome blooms could alter pelagic food webs of the northern California Current (NCC) by accelerating the biological pump via active transport, fecal pellet production and mortality events. Although aggregations of *P. atlanticum* have the potential to shape marine trophic dynamics via carbon export, little is known about pyrosome vertical distribution patterns. In this study, we estimated the distribution of *P. atlanticum* in the NCC along transects off of Oregon (45°N and 124°W) and northern California (41°N and 124°W), USA during February and July 2018. Depth-stratified plankton tows provided volume-normalized pyrosome abundance and biovolume estimates that complemented fine-scale counts by a vertically deployed camera system. Pyrosomes were numerous offshore during February, especially off Oregon. Colonies were distributed non-uniformly in the water column with peak numbers associated with vertical gradients in environmental parameters, notably density and chl-*a*. Vertical distributions shifted over the 24-h period, indicative of diel vertical migration. Understanding the vertical distribution of these gelatinous grazers in the NCC gives insight to their behavior and ecological role in biologically productive temperate ecosystems as conditions become more favorable for recurring blooms.

KEYWORDS: pyrosome; gelatinous zooplankton; California Current; vertical migration; vertical distribution

available online at academic.oup.com/plankt

INTRODUCTION

Pyrosomes are colonial pelagic tunicates comprised of hundreds or thousands of identical, millimeter-sized zooids connected by a gelatinous tunic. These cylindrical colonies can reach a maximum length of tens of centimeters to meters in length, depending on the species (Van Soest, 1981). Each zooid uses cilia to drive continuous feeding currents through an internal branchial basket; a fine-mesh mucous sheet is secreted over this structure to capture prey particles prior to ingestion (Alldredge and Madin, 1982). The zooids' excurrent siphons are oriented towards a common central cavity, open at one end, where a weakly propulsive jet of water is produced (Alldredge and Madin, 1982; Holland, 2016). Pyrosomes are among the most efficient pelagic herbivores. In high densities, *Pyrosoma atlanticum* Péron, 1804 have been documented to consume up to 95% of daily phytoplankton stock (Drits *et al.*, 1992; Henschke *et al.*, 2019). Their wide prey range includes cells >10 μm (Perissinotto *et al.*, 2007) and potentially as small as nano- and pico-plankton (Sutherland *et al.*, 2018; Thompson *et al.*, 2021). Efficient consumption of small particles allows these large grazers to "short-circuit" the microbial loop, bypassing lower trophic levels (Conley *et al.*, 2018).

Pyrosoma atlanticum is a cosmopolitan species of pyrosome, found from 50°N to 50°S, though normally uncommon in the eastern Pacific north of southern California (Van Soest, 1981). Previously, pyrosomes (not identified to species, but including *P. atlanticum* and *P. aherniosum* Seeliger, 1895) were found in almost half of the annual California Cooperative Oceanic Fisheries Investigations zooplankton surveys off southern California, with highest biomass in the "cool-phase" regime (Lavaniegos and Ohman, 2003). Before 2014, few pyrosomes had been documented in the northern California Current (NCC), a temperate portion of the California Current north of Cape Mendocino, California (Brodeur *et al.*, 2018). Unprecedented blooms of *P. atlanticum* began occurring in the NCC between 2016 and 2018, each year expanding incrementally northward along the west coast of north America (Brodeur *et al.*, 2018; Sutherland *et al.*, 2018; Miller *et al.*, 2019). In 2017, peak catches from midwater trawls off Oregon exceeded 60 000 kg km^{-3} (Brodeur *et al.*, 2018). In such high densities, pyrosomes can impact carbon cycling in the open ocean through high clearance rates and fecal pellet production (Steinberg *et al.*, 2008; Henschke *et al.*, 2019). Brodeur *et al.* (2019) suggested that the emergence of a marine heatwave (Bond *et al.*, 2015; Di Lorenzo and Mantua, 2016) and strong El Niño (Jacox *et al.*, 2016) created the appropriate conditions for a pyrosome bloom. Understanding the distribution of *P. atlanticum* during these bloom events may provide insight into their ecological role in temperate ecosystems as conditions become more favorable for recurring blooms.

Although the spatial distribution of *P. atlanticum* in the NCC has been described during bloom years (2016–2019) along the west coast of North America (Miller *et al.*, 2019), seasonal and vertical distribution patterns have not yet been explored. The vertical structuring of plankton is often influenced by physical and biological features of the water column, particularly the thermocline and subsurface chlorophyll maximum (Townsend *et al.*, 1984; Sameoto, 1986; Harris, 1988). In the Eastern Atlantic and tropical Pacific, pyrosomes have been documented undergoing large daily vertical migrations to nearly 1000 m (Angel, 1989; Andersen *et al.*, 1992; Henschke *et al.*, 2019). To date, the only study describing the vertical distribution of *P. atlanticum* in the Pacific occurred in the Tasman Sea (Henschke *et al.*, 2019). Vertically migrating zooplankton can accelerate the biological pump through the physical transport of material to depth (i.e. "eat high, poop low"), impacting how carbon is sequestered in the deep ocean (Steinberg *et al.*, 2008). If *P. atlanticum* in the NCC perform similar migrations, the collective effect on carbon export may be enhanced.

Quantifying diel vertical migration (DVM) is a challenge as it requires capturing movements over fine temporal and spatial scales. The distribution of zooplankton is often vertically patchy, forming thin, distinct layers in association with the physical structure of the water column (McManus *et al.*, 2003). Pelagic tunicates, specifically, may aggregate in layers <2-m thick (Paffenhöfer *et al.*, 1991). Traditional and depth-stratified sampling methods (i.e. net tows) lack the resolution needed to identify detailed vertical structure over a large depth range. *In situ* camera counts can resolve the location of pyrosome layers to the meter scale and have been used previously to quantify vertical distribution of gelatinous zooplankton (Silguero and Robison, 2000; Bi *et al.*, 2013; Stenvers *et al.*, 2021).

The aim of this study was to quantify how *P. atlanticum* colonies were distributed over space and time in the NCC. This broad goal was achieved by addressing the following questions: (i) Does the spatial distribution of *P. atlanticum* vary with oceanographic features? (ii) Does vertical structuring of *P. atlanticum* vary with environmental parameters? (iii) Do *P. atlanticum* in the NCC exhibit DVM? (iv) Are vertical distribution patterns consistent over time? Addressing these questions provides insight into how shifts in distribution—especially vertical position—mediate ecological impacts in a changing ecosystem.

METHODS

Sampling sites and regional oceanography

As part of the MEsoZooplankton in the CALifornia Current (MEZCAL) project, pyrosomes identified as *P. atlanticum* (Fig. 1) were sampled during winter (15–23 February 2018) and summer (3–12 July 2018) research cruises on the R/V Sikuliaq and R/V Sally Ride, respectively. Pyrosomes were sampled along transects off Newport, OR (NH; 45°N, 124°W) and Trinidad Head, CA (TR; 41°N, 124°W). Each transect had five stations extending across the continental shelf and slope (Table I and Fig. 2). Sampling occurred during both day and night, avoiding the hour before or after sunset and sunrise.

Since pyrosome distribution has been shown to occur in association with certain physical features (Henschke *et al.*, 2019; Miller *et al.*, 2019; Schram *et al.*, 2020; Stenvers *et al.*, 2021), the spatial distribution of pyrosomes may be affected by seasonal changes. Vertical CTD (SBE 911) casts to 100 m, or 5 m off the bottom when depth was < 100 m, were made at each station. Temperature (°C), salinity (PSU), density (σ_t, kg m^{-3}) and chlorophyll-*a* (chl-*a*, mg m^{-3}) measurements were averaged to 1-m bins. Mixed layer depth was calculated using the fixed density criterion ($\Delta\sigma_t = 0.125$ kg m^{-3}; Monterey and Levitus, 1997). We calculated a stratification index as previously used in zooplankton distribution studies to describe the change in seawater density between the surface and benthos (e.g. Lavaniegos and Ohman, 2003; Júnior *et al.*, 2015):

$$\text{Stratification index} = \sigma_{t,\,100\text{m}} - \sigma_{t,\,5\text{m}}$$

We used these indices to compare the numbers and distribution of pyrosomes around the pycnocline to the degree of water column stratification. We identified oceanographic conditions during the February and July cruises in 2018. Regional sea-surface temperature (SST) maps were generated from a multi-sensor Geo-Polar blended analysis (Imager+AVHRR+VIIRS) at 5-km resolution (NOAA CoastWatch/OceanWatch, Maturi *et al.*, 2017). Representative SST values were calculated from averaging cells within 10 km of each transect.

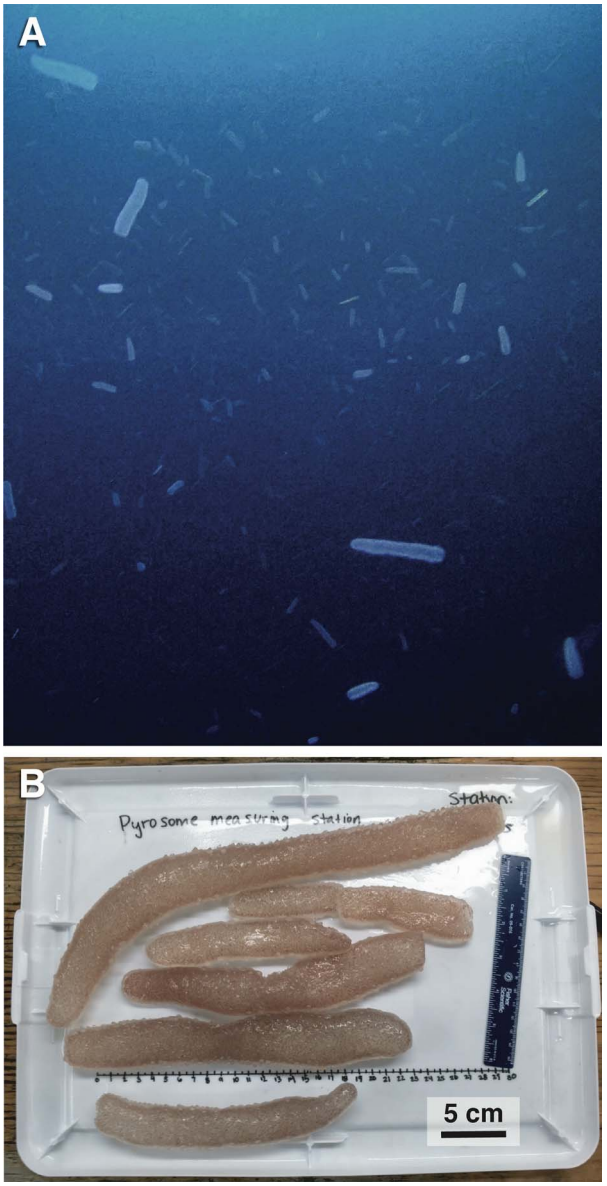

Fig. 1. Images of *Pyrosoma atlanticum* colonies sampled in 2018. (**a**) Vertically-deployed cameras recorded a dense aggregation of pyrosomes at ~45-m depth offshore of Newport, OR, USA (NH 5) in February. (**b**) Pyrosome colonies collected by MOCNESS tows in July.

Depth-stratified net tows

Pyrosoma atlanticum colonies were collected from coupled multiple opening and closing environmental sensing system (MOCNESS) tows (Guigand *et al.*, 2005; Wiebe *et al.*, 2014). The nets had openings of 1 and 4 m^2 with mesh sizes of 333 and 1000 μm, respectively. The pair of nets sampled to 100-m depth in four separate 25-m bins, and a fifth net ("net 0") was towed to 100 m during the downcast. Some stations were sampled twice within 48–72 h and in these cases average abundance is presented. Due to a malfunctioning flowmeter on some deployments, the volume filtered by each net for all stations on both cruises was calculated using the following equation: $V_{\text{filtered}} = (A_{\text{net}})(s)(t)$, where V_{filtered} is the total volume filtered, A_{net} is the area of the net opening, s is the speed through the water and t is the time elapsed. The average s, 0.786 m s^{-1}, was calculated from tows when the flowmeter was functioning properly. Because the area of the net opening fluctuates with its tow angle, we estimated

Table I: Sampling locations and bathymetric depth at stations along transects off Newport, Oregon (NH) and Trinidad Head, California (TR), USA, sampled on 15–23 February and 3–12 July 2018. The number of MOCNESS ("MOC") and camera deployments are listed for each station and cruise. Parentheses denote the number of sampling events where pyrosomes were present for each station if different from total deployment number. Depth of sampling was restricted to 100 m, or 5 m above the seafloor at shallower stations

					February 2018		July 2018	
Transect	Station no.	Latitude	Longitude	Bathymetric depth (m)	MOC	Camera	MOC	Camera
NH	1	44.652	−124.295	79	2	3	3 (2)	4 (3)
NH	2	44.652	−124.412	86	1 (0)	2 (1)	2	3
NH	3	44.652	−124.650	293	2 (1)	2	3	4
NH	4	44.652	−124.883	434	0	1	2	3
NH	5	44.652	−125.117	704	1 (0)	3	2	4
TR	1	41.058	−124.267	80	2 (0)	2 (0)	3 (1)	3 (0)
TR	2	41.058	−124.342	148	1 (0)	1 (0)	2 (1)	2 (1)
TR	3	41.058	−124.433	462	2	2 (1)	4 (3)	3 (2)
TR	4	41.058	−124.583	763	0	0	2	2
TR	5	41.058	−124.750	870	2 (0)	2 (1)	3 (2)	3 (2)

this value:

$$A_{\text{net}} = (A_{45^\circ})\left(\frac{\cos(\theta_{\text{avg}})}{\cos(45^\circ)}\right)$$

where A_{net} is the area of the net opening, A_{45° is the nominal net area (1 and 4 m^2 at 45°) and θ_{avg} is the average instrument angle. Pyrosome colonies in each net were enumerated and their volume measured by displacement. Biovolume (mL m^{-3}) was calculated by dividing the total pyrosome volume by the volume of water sampled in that tow. If pyrosomes were too numerous to count, a subset of 20 from each depth bin were measured for biovolume. Colony lengths were only measured during July 2018.

CTD-mounted camera

We mounted a GoPro Hero 4 (4K, 30fps) in a deep-water housing (GoDeep Aluminum, Sexton Inc.) and two 7500 lumen lights (BigBlue VL7500P) to the ship's onboard CTD rosette frame. At each station, simultaneous CTD and camera deployments captured fine-scale (1 m), *in situ* counts of pyrosomes to 100 m, or 5-m above the bottom at shallower stations, along with environmental data (i.e. temperature, salinity and chl-*a*). A stopwatch was used to synchronize the camera to the start of data logging on the CTD sensors. Camera frames were subsequently analyzed to determine pyrosome distributions with depth. For each meter of depth, we extracted a still frame from the camera and counted all pyrosome colonies (Fig. 1a). Occasionally, colonies were visible in consecutive frames, verified by video playback. To avoid double-counts, we adjusted the measurement by subtracting colonies that were counted in the still frame of the previous meter. We identified the vertical distribution of colonies relative to features of the water column captured from the CTD sensors, and these relationships were used to compare distribution patterns across sampling stations.

Vertical distribution and DVM

We used fine-scale counts from camera profiles and volume-normalized abundances from MOCNESS tows to identify variation in vertical distribution. To test the relationship between vertical pyrosome distribution and chl-*a*, we compared the depth at which the maximum count of pyrosome colonies occurred from camera profiles (i.e. the statistical mode) to the depth of the chlorophyll maximum (identified from fluorometer profiles) via linear regression.

Weighted mean depth (WMD) is a common way to assess the vertical position of zooplankton relative to depth-varying environmental parameters (Andersen *et al.*, 1992; Júnior *et al.*, 2015; Henschke *et al.*, 2019; Stenvers *et al.*, 2021). WMD considers colony biovolume (as a proxy for biomass) to approximate the center of mass of colonies in the water column. WMD was calculated using the following equation:

$$\text{WMD} = \frac{\Sigma\,(b_i * d_i)}{\Sigma\,b_i}$$

where b_i is pyrosome biovolume (mL m^{-3}) and d_i is the midpoint (m) of the depth stratum sampled (i). We tested differences in day–night pyrosome colony abundance in MOCNESS depth strata using a two-way analysis of

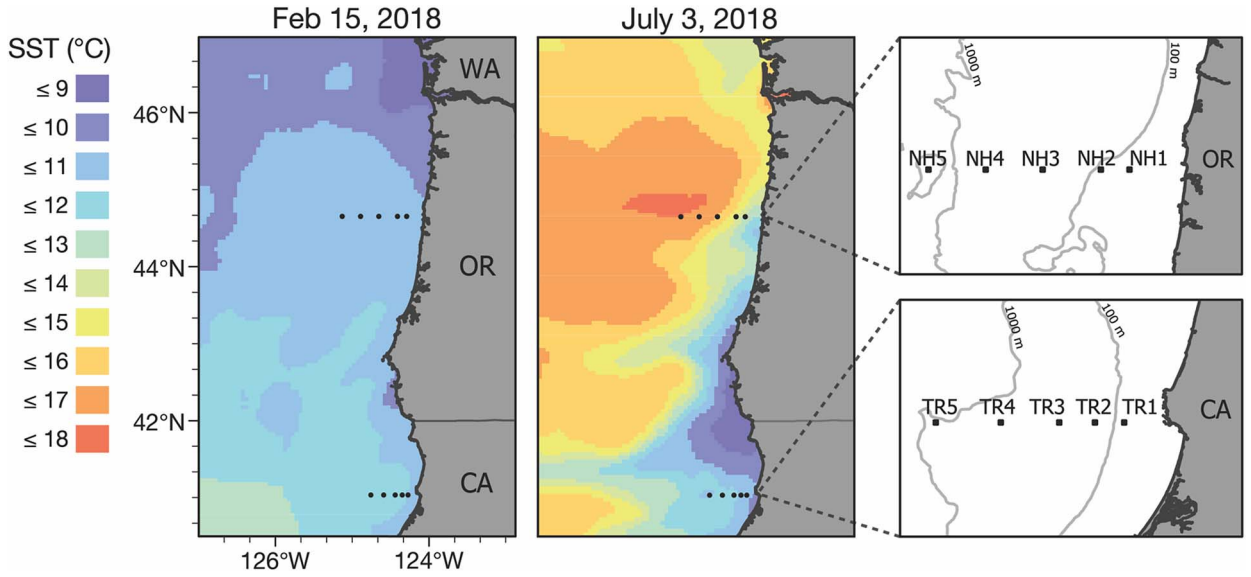

Fig. 2. Regional SST offshore of Oregon and northern California on 15 February 2018 and 3 July 2018. SST data sourced from NOAA/OceanWatch Geo-Polar Blended (imager+AVHRR+VIIRS; 5-km resolution). Study area and sampling stations off Newport, Oregon (NH) and Trinidad Head, California (TR) shown in righthand panels. Gray contours show 100 and 1000-m isobaths. See Table I for precise bathymetric depths by station.

variance (ANOVA; Type III sum of squares). *In situ* camera profiles provided finer scale vertical distribution data (1-m depth bins) than MOCNESS nets (25-m depth bins). To compare camera profiles, we identified the mode pyrosome depth—that is, the depth at which the most colonies occur—for each camera deployment. We excluded profiles where the count at the mode depth was fewer than two colonies.

RESULTS

Oceanographic conditions

Oceanographic conditions varied between February and July 2018. In February, SST was relatively cool across the study region, with temperatures of ~11°C in the vicinity of the northern transect and ~12°C near the southern transect (Fig. 2). On 3 July 2018, SSTs were higher along the northern transect (18.00 ± 0.35°C; mean ± standard deviation [SD], $n = 71$) than the southern transect (13.84 ± 0.48°C; mean ± SD, $n = 51$) based on averaging cells within 10 km of each transect. Cooler water south of Cape Blanco, Oregon was indicative of upwelling (Fig. 2).

In February, the mixed layer depth was 20.0 ± 9.5 m (mean ± SD, $n = 11$) at NH stations and 24.0 ± 9.1 m (mean ± SD, $n = 7$) at TR stations, and the chl-*a* profile was variable and distributed throughout the mixed layer, decreasing with depth (Fig. 3a–f). In July, the mixed layer depth was shallower at the NH stations (11.1 ± 4.1 m; mean ± SD, $n = 18$), and a single subsurface chl-*a* maximum was common, particularly at offshore stations (Fig. 3g–l). The mixed layer depth at most summer TR stations was similarly shallow (11.5 ± 4.1 m; mean ± SD, $n = 12$), and the chl-*a* profile was often multimodal (Supplementary Fig. S1). The fixed density criterion used in the mixed layer depth calculation did not perform as well for the gradual increases in density in some winter profiles (e.g. Fig. 3).

Water column stratification varied significantly between cruises and transects (one-way ANOVA, $F_{3,44} = 37.14$, $P < 0.0001$). Post-hoc analysis (Tukey's HSD) showed that summer stations on transect NH were primarily responsible for this result, and that winter NH and TR stations (regardless of season) were statistically indistinguishable. The stratification index on transect NH increased from winter (1.48 ± 0.58 kg m^{-3}; mean ± SD, $n = 11$) to summer (3.12 ± 0.96 kg m^{-3}; mean ± SD, $n = 18$). Stratification was lower on transect TR and did not significantly increase between winter (0.68 ± 0.17 kg m^{-3}; mean ± SD, $n = 6$) and summer (0.79 ± 0.40 kg m^{-3}; mean ± SD, $n = 13$).

Seasonal and spatial patterns in pyrosome abundance

In general, there were more pyrosome colonies observed during the winter cruise than the summer cruise but biovolume was similar between cruises (Table II) owing to apparently smaller colonies during winter (qualitative observation). *Pyrosoma atlanticum* colonies were not

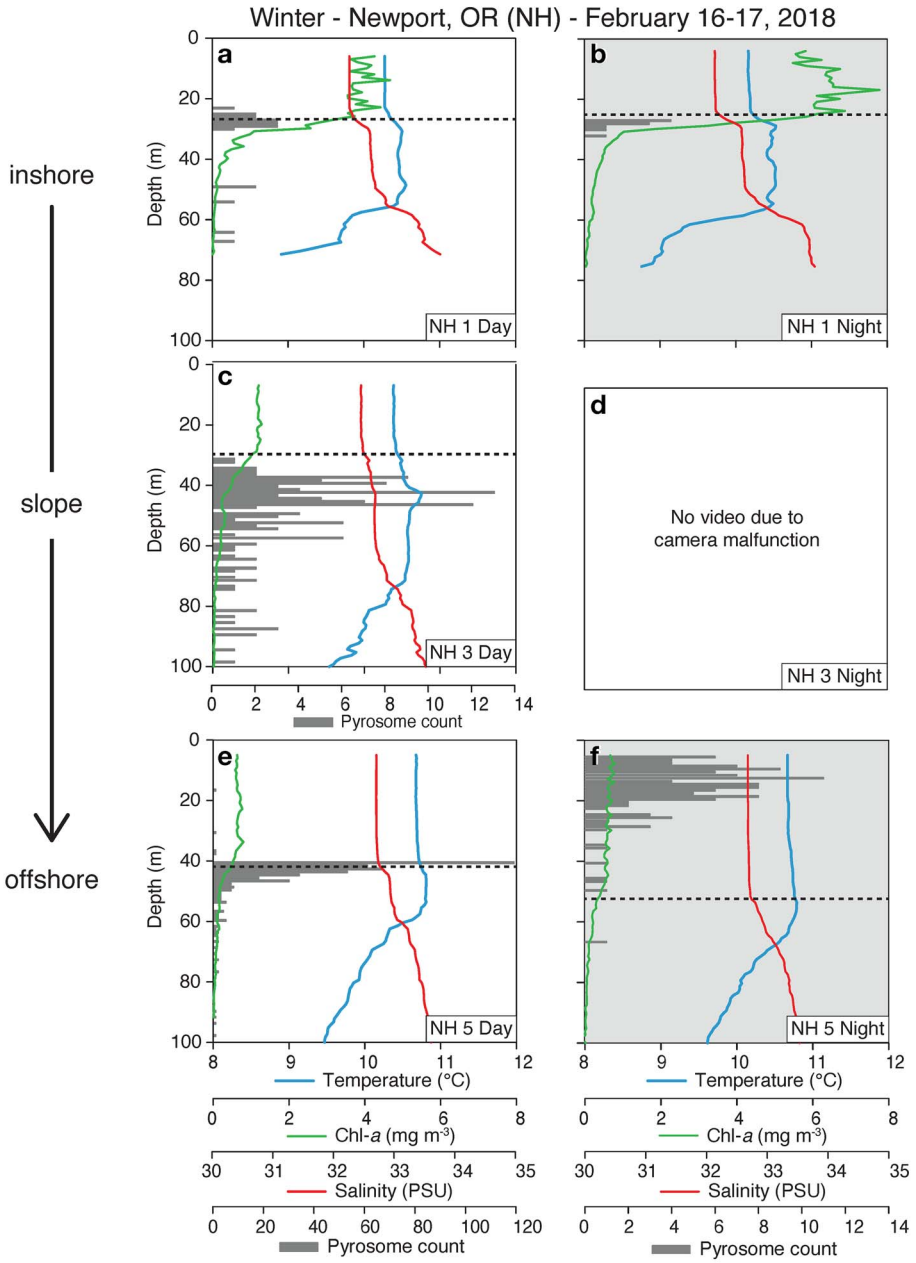

Fig. 3. Selected camera and environmental profiles from 16–17 February 2018 (**a**–**f**) to 9–10 July 2018 (**g**–**l**) on NH transect. Environmental variables (lines) shown include temperature (blue), chl-*a* (green) and salinity (red). Pyrosome counts are displayed as horizontal bars (note different scale for NH 5 day, e). Nighttime profiles are shaded. Estimated mixed layer depth is indicated by a dashed horizontal line. No video data was captured at NH3 Night (f) due to a camera malfunction.

distributed uniformly over geographic space (Fig. 4). On both winter and summer cruises, pyrosome abundance and biovolume generally increased from inshore to offshore (Table II and Fig. 4). The inshore stations on both transects (NH1 and TR1) had the lowest recorded abundances. During summer, the highest abundance (137 colonies 1000 m^{-3}) and biovolume (11.4 mL m^{-3}) were recorded during a nighttime tow at station NH5 within 25 m of the surface. Similarly, summed counts from camera profiles were highest at station NH5 in winter (454 colonies) and summer (48 colonies). The maximum camera count at any given meter interval during winter occurred at station NH5 (40 m, 119 colonies) and the maximum count during summer occurred at station

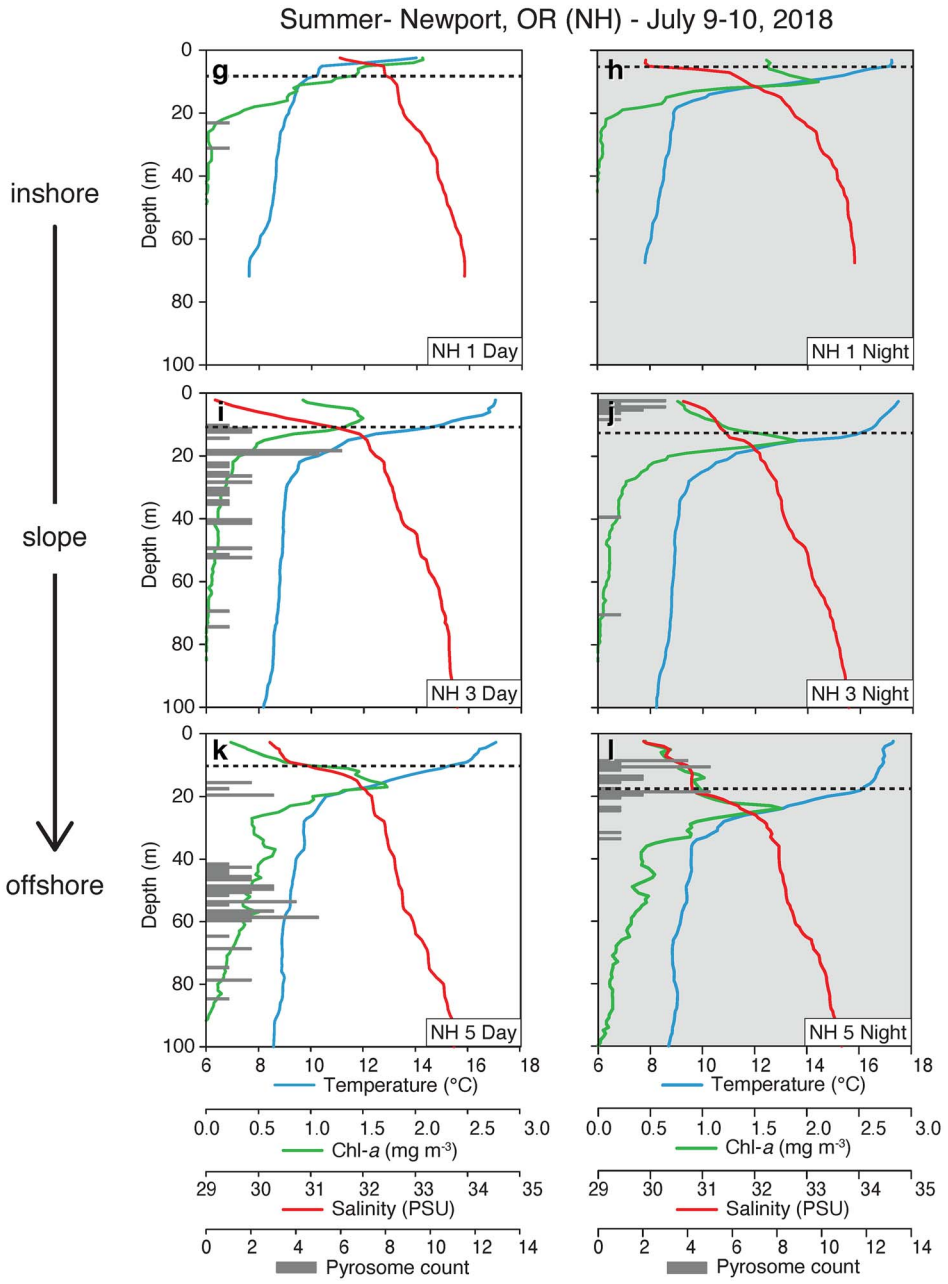

Fig. 3. Continued

NH3 (18 m, 6 colonies; Fig. 3a and b). Along the NH line, there was variability between sampling events at the same stations that were sampled twice during both February and July (Supplementary Fig. S1). Few pyrosomes were observed in nets or camera profiles on the southern transect off Trinidad Head, CA (Fig. 4 and Supplementary Fig. S1).

The colony size structure varied significantly based on sampling location in July 2018 (one-way ANOVA, $F_{2,318} = 20.6$, $P < 0.0001$; Fig. 5). Colony sizes shifted from inshore (NH1 and NH2) to offshore (NH4 and NH5): pyrosomes caught inshore were significantly larger (18.1 ± 4.6 cm; mean $\pm$ SD, $n = 49$) than offshore colonies (14.6 ± 4.4 cm; mean $\pm$ SD, $n = 229$; Tukey HSD, $P < 0.0001$). Too few colonies were caught inshore on the TR transect for meaningful a comparison. The mean colony size on transect TR (18.9 ± 7.3 cm; mean $\pm$ SD, $n = 43$) was indistinguishable from those

Table II: Mean abundance (colonies m^{-3}) and biovolume (mL m^{-3}) of P. atlanticum from MOCNESS net 0 (downcast) at sampling stations off Newport, Oregon (NH) and Trinidad Head, CA (TR) in February and July 2018. Standard deviation of the mean (SD) and number of samples (N) shown where applicable. Dashes indicate no samples collected

	February 2018						July 2018					
Station	Abundance (colonies m^{-3})	SD	*N*	Biovolume (mL m^{-3})	SD	*N*	Abundance (colonies m^{-3})	SD	*N*	Biovolume (mL m^{-3})	SD	*N*
NH1	0.041	–	1	0.37	0.088	2	0.0014	–	1	0.070	–	1
NH2	–	–	–	–	–	–	0.0052	0.0027	3	0.35	0.31	3
NH3	0.070	–	1	1.0	0.22	2	0.0093	0.0051	6	0.47	0.38	6
NH4	–	–	–	–	–	–	0.0038	0.0027	4	0.23	0.17	4
NH5	0.040	–	1	0.81	0.13	2	0.023	0.018	4	1.26	0.95	4
TR1	0	0	2	0	0	2	–	–	–	–	–	–
TR2	0	0	1	0	0	1	–	–	–	–	–	–
TR3	0.00030	0.00010	2	0.0082	0.0076	2	0.0017	0.0021	3	0.12	0.13	3
TR4	–	–	–	–	–	–	0.0022	0.0004	2	0.18	0.15	2
TR5	0	0	2	0	0	2	–	–	–	–	–	–

caught inshore on transect NH (Tukey's HSD, $P = 0.74$). Colony lengths were not measured during February 2018.

Vertical distribution and DVM

Camera profiles showed that pyrosomes were distributed non-uniformly through the water column. Colonies were often clustered near the base of the surface mixed layer (Fig. 3). Wintertime distributions tended to form distinct layers, presumably due to the higher numbers of colonies relative to summer (Figs 3 and 6). The distribution at winter station NH5 was a particularly striking example of vertical patchiness because we observed a peak of 119 colonies at 40-m depth, whereas fewer than 3 total colonies were detected at shallower depths (Fig. 3e). We rarely observed pyrosomes within 5 m of the surface. At several stations, we observed aggregations of pyrosomes around the base of the surface mixed layer and chl-*a* maximum. Although colonies appeared to be distributed near the chl-*a* maximum (Fig. 3), there was no significant linear relationship between the mode pyrosome depth and depth of chl-*a* maximum during daytime ($R^2 = 0.0014$, $df = 12$, $P = 0.90$) or nighttime ($R^2 = 0.11$, $df = 8$, $P = 0.33$) camera deployments.

Comparisons of day and night camera profiles on transect NH indicated DVM behavior. The average mode pyrosome depth in February and July was shallower at night (18.7 ± 3.0 m; mean ± SE, $n = 10$) than during the day (36.6 ± 3.5 m; mean ± SE, $n = 14$). In February, both daytime and nighttime distributions were shallow at inshore stations NH1 and NH2. Distributions were deeper during the day than at night at the offshore station NH5 (Fig. 6a). In July, daytime distributions of colonies were deeper than at night and varied across a wide depth range, whereas nighttime distributions were shallow, and encompassed a relatively narrow depth range (Fig. 6b). Too few pyrosomes were observed on TR in February to discern changes in vertical distributions. In July, the distribution of pyrosomes along TR was generally deeper than along NH (Fig. 6c).

The WMD of colonies collected from MOCNESS tows during July reinforced that the distribution of *P. atlanticum* colonies shifted towards the surface at night. They were, on average, located deeper in the water column during the day (39.0–52.4 m; 95% CI, $n = 53$) than at night (10.2–21.9 m; 95% CI, $n = 16$) at all stations on both transects during July 2018. The day–night depth shift was most pronounced at offshore stations on transect NH (Fig. 7). On transect TR, this pattern was not as clear, possibly due to overall lower colony abundances (Fig. 7). Although the abundance of pyrosomes in the 100 m sampling range did not change significantly between day and night (two-way ANOVA; $F = 0.66$, $P = 0.42$, $df = 1$), the time of sampling had a significant effect on the distribution of colonies among the depth bins ($F = 8.02$, $P < 0.001$, $df = 3$). WMD could not be calculated for the February cruise due to a malfunction in the net opening mechanism on several nighttime tows.

Comparison of sampling gear

The vertically-deployed camera reliably detected *P. atlanticum* colonies to enable comparison to the MOCNESS tows. Of 37 sampling stations that had both camera and net deployments (Table I), 31 stations showed agreement between the sampling gear, where the presence of colonies on camera corresponded to their presence in the nets. Only in three sampling events where

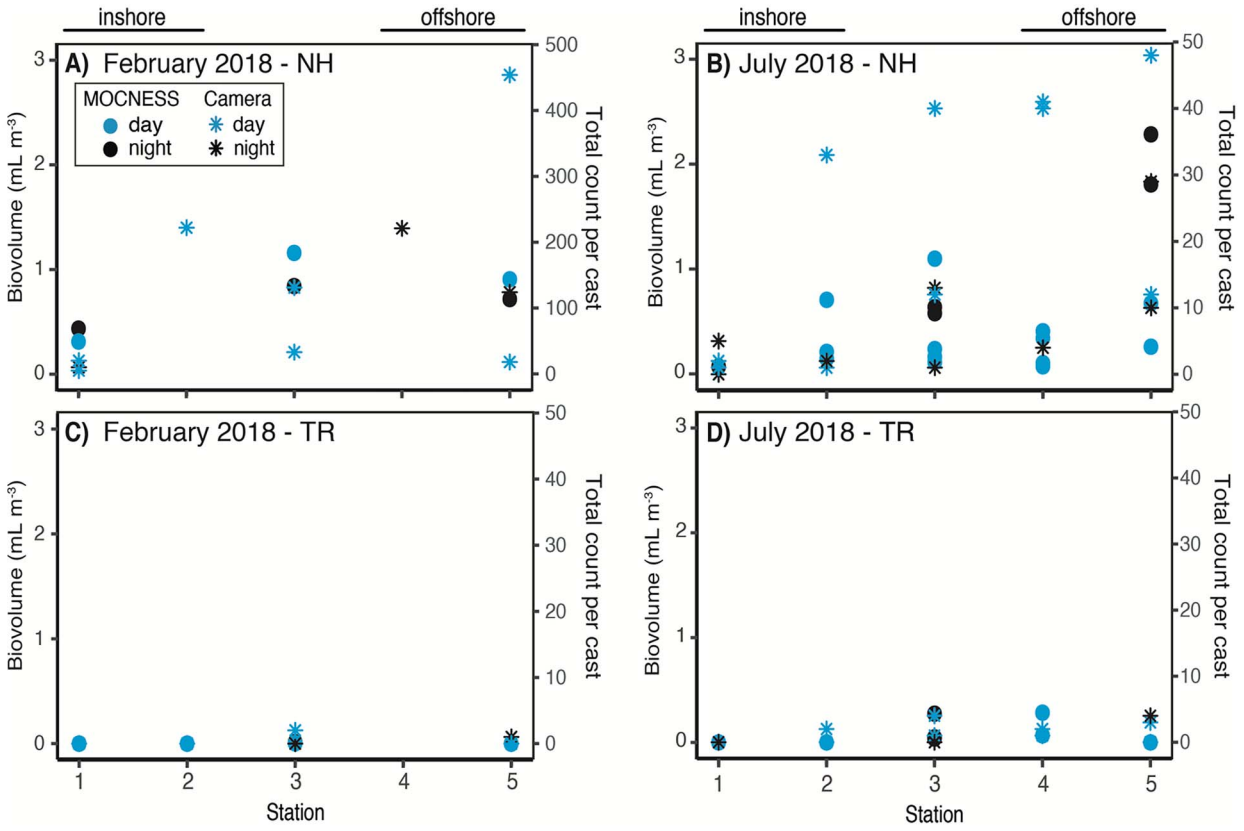

Fig. 4. Spatial distribution of *P. atlanticum* by station on the Newport, OR (NH) transect (**a**, **b**) and Trinidad Head (TR) transect (**c**, **d**) in February and July, 2018. Biovolume (mL m^{-3}) from MOCNESS net 0 are denoted by filled circles. Counts from vertically-deployed cameras are summed by cast and displayed as asterisks (note different scales for February and July on transect NH). Color represents time of deployment: night (black) and day (blue).

pyrosomes were in low densities (≤4 colonies per cast) did we see pyrosome colonies on camera but did not collect them in the nets. Similarly, there were only three instances where we saw colonies (≤3) in the nets, but not on camera. In July, daytime camera profiles at NH stations tended to have higher total counts than nighttime casts (Figs. 3a and 4b).

The oblique tows to 100 m (MOCNESS net 0) tended to underestimate pyrosome abundance relative to the cumulative 25-m increment, depth-stratified tows, particularly when there were many colonies (>30) in a given tow (Supplementary Fig. S2). Vertical patchiness or differences in sampling physics (i.e. orientation of the net relative to flow during upcast versus downcast) could explain this discrepancy (Burd and Thomson, 1993).

DISCUSSION

Despite its global distribution, little is understood about the basic biology and vertical dynamics of *P. atlanticum*. Identifying distribution patterns and migratory behaviors is key to understanding how pyrosomes fit into marine ecosystems, particularly given recent evidence of a northward range expansion in the NCC as well as anomalous blooms in other regions (Archer *et al.*, 2018; Sutherland *et al.*, 2018; Miller *et al.*, 2019; O'Loughlin *et al.*, 2020; Stenvers *et al.*, 2021). Our findings suggest that blooms of *P. atlanticum* in the NCC may have had the most prominent effects offshore and north of Cape Blanco where colony abundances were highest. The lower number of pyrosomes in the vicinity of northern California was likely related to offshore export driven by strong, continuous upwelling. Colonies underwent DVM and were associated with depths of locally elevated chlorophyll and density gradients at the base of the surface mixed layer.

Seasonal and spatial patterns in pyrosome abundance

Pyrosome distribution and size structure varied over space and time in the NCC during February and July 2018. In general, pyrosome abundances were higher at offshore stations than inshore (Fig. 7). However, the overall abundance of pyrosomes we observed decreased dramatically between the February and July cruises (Table II).

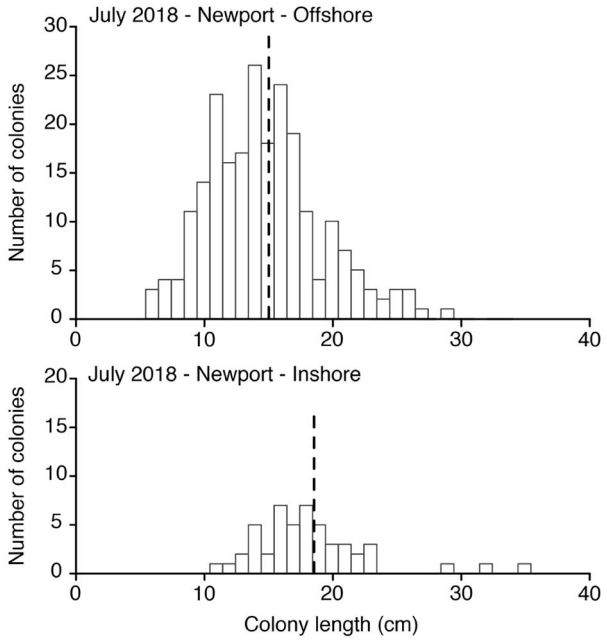

Fig. 5. Colony length distribution (in centimeters) from offshore (top, NH4 & NH5) and inshore (bottom, NH1 & NH2) stations in July 2018. Pyrosome colonies caught offshore were smaller (14.6 ± 0.3 cm; mean ± SE, $n = 229$) than inshore colonies (18.1 ± 0.7 cm; mean ± SE, $n = 49$). The vertical dotted line represents mean colony size for each group.

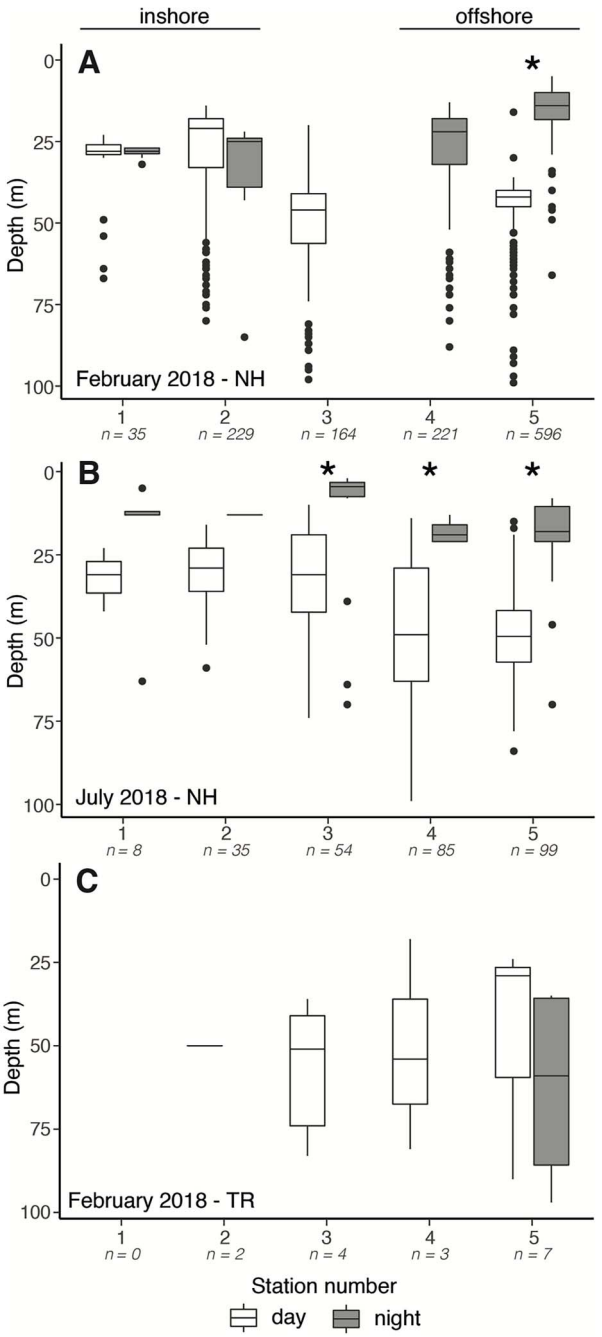

Fig. 6. Daytime (white) and nighttime (gray) distribution of pyrosome colonies from camera profiles. Pyrosome distributions from Newport, Oregon (NH) transect are shown for February (**a**) and July (**b**). Note that in winter, stations NH3 and NH4 do not have day-night pairs due to camera malfunction and lack of daytime deployment, respectively. (**c**) Pyrosome distribution from Trinidad Head, California (TR) transect are shown for July. Nighttime tows were only performed at stations TR3 and TR5, and none were observed at station TR3. Zero pyrosomes were observed at station TR1. Significant differences in day-night distribution pairs are denoted with an asterisk (one-way ANOVA, $P < 0.02$).

Changes in environmental parameters could account for this decrease as pyrosome density is positively correlated to SST and surface salinity in the NCC (Schram *et al.*, 2020). In the context of the multi-year blooms, this study occurred during the bloom slow-down. Indeed, by early the following year, there were few pyrosomes in the NCC (Miller *et al.*, 2019; O'Loughlin *et al.*, 2020). Only a single colony was caught in our nets in March 2019 (personal observation).

The NCC is an eastern boundary current system characterized by variable wind-driven upwelling (Checkley and Barth, 2009). Oceanographic conditions off Oregon's central coast are dependent on seasonal winds, which drive summer upwelling, whereas upwelling is typically more continuous in the region between Cape Blanco and Cape Mendocino (Longhurst, 2007). There is evidence that these dynamics are shifting due to climate change (Brady *et al.*, 2017). Environmental conditions associated with weak upwelling appear to be more favorable to pyrosome blooms in the NCC (O'Loughlin *et al.*, 2020; Schram *et al.*, 2020). Considerably more pyrosomes were observed off Oregon than off northern California (Table II and Fig. 4). Water column stratification appeared to be the main physical factor that differentiated

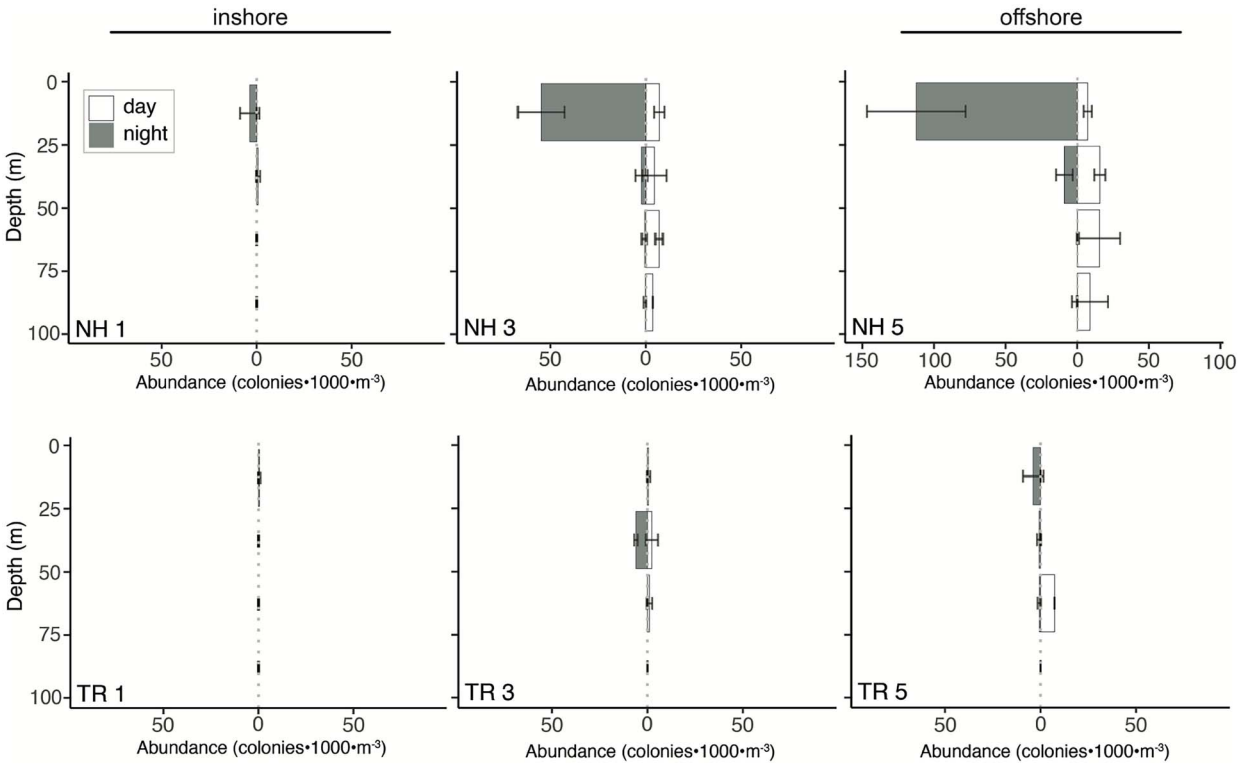

Fig. 7. Average daytime and nighttime pyrosome colony abundances (colonies m^{-3}) from MOCNESS displayed by station (left: offshore, middle: slope and right: inshore) and transect (top: NH, bottom: TR) in July 2018. Error bars represent SD. Depth bins are in 25-m vertical increments between 0 and 100-m depth.

the transects. Low stratification, as was frequently observed in this study, could indicate vertical mixing within surface waters, preventing the formation of phytoplankton layers (Chiswell *et al.*, 2014) that grazers may rely on to efficiently capture food (Benoit-Bird and McManus, 2012). However, low stratification off Oregon in February did not appear to negatively affect pyrosome layering (Fig. 3). Off-shelf export of water off northern California may explain the persistence of both low stratification and low pyrosome numbers across seasons along the TR transect (Hickey and Banas, 2008).

Stable isotope analysis suggested that pyrosome colonies collected in the NCC in 2017 grew and assimilated carbon offshore (Schram *et al.*, 2020). Thus, colonies collected at inshore stations may have been transported by advection onto the shelf. Pyrosome colonies grow through asexual budding of additional zooids over time, and new colonies are formed by sexual generation of tetrazooids (Holland, 2016). Miller *et al.* (2019) proposed that the presence of small colonies may play a key role in seeding and maintaining blooms off the west coast of North America. The increased frequency of relatively smaller (i.e. younger) colonies observed offshore (Fig. 5) may indicate that sexual reproduction occurs far from shore. Although offshore colonies were small relative to those caught inshore in July 2018, they were large (>140 mm) in the context of the Miller *et al.* (2019) study. This lack of small (<40 mm), newly budded colonies may have foreshadowed the bloom cessation in the coming months. The colony sizes we observed fell into the same range as studies in the same region in May 2017 (Schram *et al.*, 2020) and May 2018 (O'Loughlin *et al.*, 2020). O'Loughlin *et al.* (2020) observed a shift in colony size structure between February and September, 2018, with largest colonies occurring in late spring.

Vertical distribution

Pyrosoma atlanticum colonies were distributed non-uniformly in the water column with highest colony densities frequently associated with the base of the surface mixed layer, near the subsurface chlorophyll maximum (Fig. 3). Although colonies aggregated near chl-*a* peaks at night, their distribution did not correspond to the precise location of maximum chl-*a*, consistent with other observations of grazers aggregating above or below phytoplankton thin layers (Briseño-Avena *et al.*, 2020). Vertical position is likely influenced by multiple interacting factors, and gradients in food concentration may be a more important driver than peaks. Interestingly,

we rarely observed pyrosomes within the top 5 m, suggesting some surface avoidance, perhaps due to wave driven turbulence (Incze *et al.*, 2001). Our observations represent snapshots of the vertical distribution of colonies, and it is likely that the vertical positioning is the dynamic result of collective behavior interacting with physical features.

The association of colonies with the mixed layer and depths where chl-*a* is locally elevated suggests that pyrosomes target photosynthetic prey taxa. Previous studies have demonstrated grazing on diatoms, dinoflagellates, prymnesiophytes and picoeukaryotes (Perissinotto *et al.*, 2007; Schram *et al.*, 2020; Thompson *et al.*, 2021). However, high chl-*a* was not strictly associated with increased pyrosome densities (O'Loughlin *et al.*, 2020; Schram *et al.*, 2020). Pyrosomes may deplete chl-*a* locally through grazing or avoid high chl-*a* depths. The mucous-mesh of the pyrosome feeding mechanism can capture a large range of microbial prey, particularly cells > 10 μm (Perissinotto *et al.*, 2007; Thompson *et al.*, 2021). However, an overabundance of phytoplankton prey (as occurs during seasonal upwelling) may become detrimental as the mucous filters of pelagic tunicates can become clogged (Harbison *et al.*, 1986). Our results are consistent with findings from another regional study that pyrosome densities peak in late winter (O'Loughlin *et al.*, 2020) ahead of the spring transition when larger phytoplankton taxa typically become increasingly abundant (Checkley and Barth, 2009). These results could be explained by the concept that phytoplankton makeup may be important in explaining pyrosome distributions.

There are likely multiple passive and active aggregating mechanisms contributing to pyrosome colony clustering in the water column. A previous study of doliolids, another pelagic tunicate, concluded that aggregations were the result of directional swimming and rarely coincided with depths of high chlorophyll concentrations (Paffenhöfer *et al.*, 1991). Sharp salinity gradients can be a physical barrier to the migration of small zooplankton (Lougee *et al.*, 2002), although it is unclear whether these density gradients affect pyrosome swimming. Some gelatinous zooplankton aggregate around haloclines as a behavioral preference (Arai, 1973), but to our knowledge no one has studied pyrosome swimming dynamics in enough detail to evaluate whether pyrosomes exhibit similar behavior. Unfortunately, difficulty in keeping pyrosomes in captivity and a lack of *in situ* swimming observations have hampered exploration of these questions.

Diel vertical migration

WMD analysis revealed a nighttime vertical shift of *P. atlanticum* colonies towards the surface. DVM is likely the mechanism driving these changes in vertical structure, although the scale of migrations by NCC pyrosomes remains unclear. Because our sampling was limited to the top 100 m of the water column, we could only determine the position of colonies relative to the surface between day and night. We observed similar colony biovolume within the 100-m sampling depth at night relative to the day, with the exception of summer station NH5 where the nighttime biovolume increased (Fig. 4b). Except for colonies sampled at shallow inshore stations (<100 m of water column depth), we cannot rule out the possibility that *P. atlanticum* is performing migrations over hundreds of meters, similar to those shown in studies elsewhere in the world (Angel, 1989; Andersen *et al.*, 1992; Henschke *et al.*, 2019).

DVMs may be the result of several mechanisms including light-avoidance, feeding and reproduction. *Pyrosoma atlanticum*, like other vertically migrating zooplankton, may migrate up to the chlorophyll maximum at night (Harris, 1988) to feed in darkness, safe from visual predators (Lampert, 1989). Due to phytoplankton bloom shadowing, light may more readily penetrate clear, oligotrophic waters of the tropics than the particle-filled waters of the NCC (Kaartvedt *et al.*, 1996; Sato *et al.*, 2013). Although our observations were constrained to the upper 100 m, the scale of the pyrosome downward migrations we observed within those depths may be less extensive because the hypothesized migration cue (i.e. light) is relatively reduced near the surface. Henschke *et al.* (2019) concluded that chl-*a* levels were driving vertical distribution patterns of *P. atlanticum*; in a cold-core (upwelling) eddy, pyrosome colonies were distributed closer to the surface, remaining in the top 100 m during the day. Finally, pelagic tunicates may aggregate to increase gamete concentrations during reproductive events (Purcell and Madin, 1991).

High grazing rates by NCC pyrosomes in surface waters and gut turnover of >2.5 h (O'Loughlin *et al.*, 2020) combined with daytime migration to depths could expedite carbon export via active transport (Steinberg *et al.*, 2008). Thus, large aggregations of vertically migrating pyrosomes have the potential to alter NCC trophic dynamics by short-circuiting the microbial loop and accelerating the biological pump. Pyrosomes and other pelagic tunicates use mucous-mesh sieving to harvest small particles, removing available food for micro- and meso-zooplankton in surface waters, termed a "short-circuit" as it bypasses those lower trophic levels (Le Fèvre *et al.*, 1998; Pomeroy *et al.*, 2007; Conley *et al.*, 2018). Recent estimates indicate that active transport by *P. atlanticum* has a minimal impact when the mixed layer is deep (>180 m; Henschke *et al.*, 2019), but may play a bigger role in the NCC where mixed layer depth is often

much shallower. Aggregations of pyrosomes may quickly assimilate carbon in surface waters and then migrate to depth where they produce fecal pellets or are themselves ingested by mesopelagic or benthic consumers. These effects may be more pronounced offshore where colony abundances were higher and there is greater potential for pyrosome biomass to be transported to depth.

Comparison of sampling gear

The vertically deployed camera system was a reliable and cost-effective method to sample the vertical structure of conspicuous, abundant macrozooplankton. Cameras provided higher resolution *in situ* counts relative to the large ship-deployed MOCNESS net system that was constrained by the number of available nets and human processors. Although we deployed the camera from the shipboard CTD rosette, this method could be easily adapted for use with smaller CTD cages deployed off boats or docks. We limited sampling to the top 100 m of the water column, but sampling depth could be increased or expanded through use of shipboard acoustic backscatter to capture deep distributions and migration speeds (Henschke *et al.*, 2019).

The main drawback of single-camera methods is unknown sampling volume, without which calculating normalized abundance is impossible. This may be a particular issue in comparing counts from camera profiles under different lighting regimes. The additional light from surface illumination during daytime camera profiles may increase visibility of distant colonies relative to nighttime (or deep) casts lit only by the mounted lights. One could reasonably create and apply a correction factor based on background light intensity and attenuation. The limitation of a single camera could also be addressed by mounting cameras to nets (Stenvers *et al.*, 2021) or underwater vision profilers (UVPs; Hoving *et al.*, 2019) with known sampling volume. Deploying calibrated stereo cameras where distance in three-dimensional space is measurable would also allow for *in situ* abundance calculations (Goetze *et al.*, 2019). However, the single camera was sufficient to identify distribution patterns and make comparisons between deployments.

Implications for the NCC

Large blooms of *P. atlanticum* similar to those seen in 2018 could affect pelagic food webs of the NCC due to increased grazing pressure (Drits *et al.*, 1992; Henschke *et al.*, 2019; O'Loughlin *et al.*, 2020; Thompson *et al.*, 2021) that may restructure energy transfer. Recent estimates suggest that NCC pyrosomes could consume almost a quarter of daily phytoplankton standing stock (O'Loughlin *et al.*, 2020). Consequently, pyrosome feeding at a low trophic level could decrease the amount of food available to other zooplankton grazers in surface waters of the NCC (Conley *et al.*, 2018; O'Loughlin *et al.*, 2020; Schram *et al.*, 2020). However, pyrosome biomass is not a trophic dead-end. Pyrosomes have higher energy content per g wet mass than cnidarian jellyfish (Doyle *et al.*, 2007), and pelagic fish and cetaceans have been recorded feeding on NCC pyrosomes (Brodeur *et al.*, 2018, 2021). In addition, jelly-falls composed of *P. atlanticum* in the NCC provide extra carbon input to benthic consumers such as crustaceans, sea stars, brittle stars and anemones (Lebrato and Jones, 2009; Archer *et al.*, 2018; Stenvers *et al.*, 2021). The unprecedented blooms of *P. atlanticum* in recent years are likely tied to a large-scale shift in oceanographic conditions along the US West Coast (Brodeur *et al.*, 2019). Understanding the distribution of these gelatinous grazers will give insight into their ecological role in the NCC as favorable bloom conditions become more common.

CONCLUSIONS

Distributions of *P. atlanticum* were analyzed from two expeditions in February and July of 2018 during an anomalous bloom that followed unusual regional warming events. The abundance and size structure of *P. atlanticum* colonies varied non-uniformly over space and time in the NCC. Pyrosome abundances peaked in February and tended to increase with distance from shore. Consistently low abundances off of northern California is likely related to offshore transport driven by strong, continuous upwelling currents. Pyrosome vertical distribution was variable, although high densities of pyrosomes were frequently associated with the base of the surface mixed layer, near the subsurface chlorophyll maximum. We provide initial observations of NCC pyrosomes that exhibited DVM behavior, although the scale of these migrations in the region remains unclear. Nevertheless, the daily vertical movement across environmental gradients may accelerate the biological pump via active transport of material to depth. Our observations contribute to our understanding of the role of pyrosomes in a changing ecosystem.

SUPPLEMENTARY DATA

Supplementary data can be found at *Journal of Plankton Research* online.

ACKNOWLEDGEMENTS

We thank the captains and crews of the R/V Sikuliaq and R/V Sally Ride. We also thank Hilarie Sorensen, Sandra Dorning and Matthew Gimpelevich who contributed to camera

deployments and subsequent video analysis, María José Marín Jarrín for providing protocols for CTD processing and Marco Corrales-Ugalde for draft comments. We sincerely thank two anonymous reviewers for their insight and constructive comments.

FUNDING

National Science Foundation (grants OCE-1737364 and 1851537 to K.R.S. and OCE-1737399 to R.K.C. and S.S.).

DATA ARCHIVING

Pyrosome data are archived with the Biological and Chemical Oceanography Data Management Office https://www.bco-dmo.org/project/743417.

REFERENCES

Alldredge, A. L. and Madin, L. P. (1982) Pelagic tunicates: unique herbivores in the marine plankton. *Bioscience*, **32**, 655–663.

Andersen, V., Sardou, J. and Nival, P. (1992) The diel migrations and vertical distributions of zooplankton and micronekton in the Northwestern Mediterranean Sea. 2. Siphonophores, hydromedusae and pyrosomids. *J. Plankton Res.*, **14**, 1155–1169.

Angel, M. V. (1989) Vertical profiles of pelagic communities in the vicinity of the Azores Front and their implications to deep ocean ecology. *Prog. Oceanogr.*, **22**, 1–46.

Arai, M. N. (1973) Behavior of the planktonic coelenterates, *Sarsia tubulosa*, *Phialidium gregarium*, and *Pleurobrachia pileus* in salinity discontinuity layers. *J. Fish. Res. Board Canada*, **30**, 1105–1110.

Archer, S. K., Kahn, A. S., Leys, S. P., Norgard, T., Girard, F., du Preez, C. and Dunham, A. (2018) Pyrosome consumption by benthic organisms during blooms in the Northeast Pacific and Gulf of Mexico. *Ecology*, **99**, 981–984.

Benoit-Bird, K. J. and McManus, M. A. (2012) Bottom-up regulation of a pelagic community through spatial aggregations. *Biol. Lett.*, **8**, 813–816.

Bi, H., Cook, S., Yu, H., Benfield, M. C. and Houde, E. D. (2013) Deployment of an imaging system to investigate fine-scale spatial distribution of early life stages of the ctenophore *Mnemiopsis leidyi* in Chesapeake Bay. *J. Plankton Res.*, **35**, 270–280.

Bond, N. A., Cronin, M. F., Freeland, H. and Mantua, N. (2015) Causes and impacts of the 2014 warm anomaly in the NE Pacific. *Geophys. Res. Lett.*, **42**, 3414–3420.

Brady, R. X., Alexander, M. A., Lovenduski, N. S. and Rykaczewski, R. R. (2017) Emergent anthropogenic trends in California Current upwelling. *Geophys. Res. Lett.*, **44**, 5044–5052.

Briseño-Avena, C., Prairie, J. C., Franks, P. J. S. and Jaffe, J. S. (2020) Comparing vertical distributions of chl-*a* fluorescence, marine snow, and taxon-specific zooplankton in relation to density using high-resolution optical measurements. *Front. Mar. Sci.*, **7**, 602.

Brodeur, R., Buckley, T. W., Lang, G. M., Draper, D. L., Buchanan, J. C. and Hibpshman, R. E. (2021) Demersal fish predators of gelatinous zooplankton in the Northeast Pacific Ocean. *Mar. Ecol. Prog. Ser.*, **658**, 89–104.

Brodeur, R. D., Auth, T. D. and Phillips, A. J. (2019) Major shifts in pelagic micronekton and macrozooplankton community structure in an upwelling ecosystem related to an unprecedented marine heatwave. *Front. Mar. Sci.*, **6**, 1–15.

Brodeur, R. D., Brodeur, R. D., Perry, R. I., Boldt, J., Flostrand, L., Galbraith, M., King, J., Murphy, J. *et al.* (2018) An unusual gelatinous plankton event in the NE Pacific: the Great Pyrosome Bloom of 2017. *California Mar. Ecol.*, **26**, 22–27.

Burd, B. J. and Thomson, R. E. (1993) Flow volume calculations based on three-dimensional current and net orientation data. *Deep. Res. Part I*, **40**, 1141–1153.

Checkley, D. M. and Barth, J. A. (2009) Patterns and processes in the California Current system. *Prog. Oceanogr.*, **83**, 49–64.

Chiswell, S. M., Calil, P. H. R. and Boyd, P. W. (2014) Spring blooms and annual cycles of phytoplankton: a unified perspective. *J. Plankton Res.*, **37**, 500–508.

Conley, K. R., Lombard F., Sutherland K. R. (2018) Mammoth grazers on the ocean's minuteness: a review of selective feeding using mucous meshes. *Proc. R. Soc. B Biol. Sci.*, 20180056 **285** 1878.

Di Lorenzo, E. and Mantua, N. (2016) Multi-year persistence of the 2014/15 North Pacific marine heatwave. *Nat. Clim. Chang.*, **6**, 1042–1047.

Doyle, T. K., Houghton, J. D. R., McDevitt, R., Davenport, J. and Hays, G. C. (2007) The energy density of jellyfish: estimates from bomb-calorimetry and proximate-composition. *J. Exp. Mar. Bio. Ecol.*, **343**, 239–252.

Drits, A. V., Arashkevich, E. G. and Semenova, T. N. (1992) *Pyrosoma atlanticum* (Tunicata, Thaliacea): grazing impact on phytoplankton standing stock and role in organic carbon flux. *J. Plankton Res.*, **14**, 799–809.

le Fèvre J., Legendre L., Rivkin R. B. (1998) Fluxes of biogenic carbon in the Southern Ocean: roles of large microphagous zooplankton. *J. Mar. Syst.* pp. 325–345 **17** 1–4.

Goetze, J. S., Bond T., McLean D. L., Saunders B. J., Langlois T. J., Lindfield S., Fullwood L. A. F., Driessen D., *et al.* (2019) A field and video analysis guide for diver operated stereo-video. *Methods Ecol. Evol.*, **10**, 1083–1090 7.

Guigand, C. M., Cowen R. K., Llopiz J. K., Richardson D. E. (2005) A coupled asymmetrical multiple opening closing net with environmental sampling system. *Mar. Technol. Soc. J.*, **39**, 22–24 2.

Harbison, G., McAlister V. L., Gilmer R. W. (1986) The response of the salp, *Pegea confoederata*, to high levels of particulate material: starvation in the midst of plenty. *Limnol. Oceanogr.*, **31**, 371–382 2.

Harris, R. P. (1988) Interactions between diel vertical migratory behavior of marine zooplankton and the subsurface chlorophyll maximum. *Bull. Mar. Sci.*, **43**, 663–674.

Henschke, N., Pakhomov, E. A., Kwong, L. E., Everett, J. D., Laiolo, L., Coghlan, A. R. and Suthers, I. M. (2019) Large vertical migrations of *Pyrosoma atlanticum* play an important role in active carbon transport. *J. Geophys. Res.*, **124**, 1056–1070.

Hickey, B. M. and Banas, N. S. (2008) Why is the northern end of the California Current system so productive? *Oceanography*, **21**, 90–107.

Holland, L. Z. (2016) Tunicates. *Curr. Biol.*, **26**, R146–R152.

Hoving, H. J., Christiansen S., Fabrizius E., Hauss H., Kiko R., Linke P., Neitzel P., Piatkowski U., *et al.* (2019) The pelagic in situ observation system (PELAGIOS) to reveal biodiversity, behavior, and ecology of elusive oceanic fauna. *Ocean Sci.*, **15**, 1327–1340 5.

Incze, L. S., Hebert, D., Wolff, N., Oakey, N. and Dye, D. (2001) Changes in copepod distributions associated with increased turbulence from wind stress. *Mar. Ecol. Prog. Ser.*, **213**, 229–240.

Jacox, M. G., Hazen, E. L., Zaba, K. D., Rudnick, D. L., Edwards, C. A., Moore, A. M. and Bograd, S. J. (2016) Impacts of the 2015–2016 El Niño on the California Current system: early assessment and comparison to past events. *Geophys. Res. Lett.*, **43**, 7072–7080.

Júnior, M. N., Brandini, F. P. and Codina, J. C. U. (2015) Diel vertical dynamics of gelatinous zooplankton (Cnidaria, Ctenophora and Thaliacea) in a subtropical stratified ecosystem (South Brazilian Bight). *PLoS One*, **10**, 1–28.

Kaartvedt, S., Melle, W., Knutsen, T. and Skjoldal, H. R. (1996) Vertical distribution of fish and krill beneath water of varying optical properties. *Mar. Ecol. Prog. Ser.*, **136**, 51–58.

Lampert, W. (1989) The adaptive significance of diel vertical migration of zooplankton. *Funct. Ecol.*, **3**, 21–27.

Lavaniegos, B. E. and Ohman, M. D. (2003) Long-term changes in pelagic tunicates of the California Current. *Deep. Res. Part II Top. Stud. Oceanogr.*, **50**, 2473–2498.

Lebrato, M. and Jones, D. O. B. (2009) Mass deposition event of *Pyrosoma atlanticum* carcasses off Ivory Coast (West Africa). *Limnol. Oceanogr.*, **54**, 1197–1209.

Longhurst, A. R. (2007) *Ecological Geography of the Sea*, 2nd edn, Academic Press, Burlington, MA, USA.

Lougee, L. A., Bollens, S. M. and Avent, S. R. (2002) The effects of haloclines on the vertical distribution and migration of zooplankton. *J. Exp. Mar. Bio. Ecol.*, **278**, 111–134.

Maturi, E., Harris, A., Mittaz, J., Sapper, J., Wick, G., Zhu, X., Dash, P. and Koner, P. (2017) A new high-resolution sea surface temperature blended analysis. *Bull. Am. Meteorol. Soc.*, **98**, 1015–1026.

McManus, M. A., Alldredge, A. L., Barnard, A. H., Boss, E., Case, J. F., Cowles, T. J., Donaghay, P. L., Eisner, L. B. *et al.* (2003) Characteristics, distribution and persistence of thin layers over a 48 hour period. *Mar. Ecol. Prog. Ser.*, **261**, 1–19.

Miller, R. R., Santora, J. A., Auth, T. D., Sakuma, K. M., Wells, B. K., Field, J. C., Brodeur, R. D. (2019) Distribution of pelagic Thaliaceans, *Thetys vagina* and *Pyrosoma atlanticum*, during a period of mass occurrence within the California Current. *CalCOFI Rep.*, **60**, 1–15.

Monterey, G. and Levitus, S. (1997) Seasonal variability of mixed layer depth for the world ocean. *NOAA Atlas NESDIS*, **14**, 96.

O'Loughlin, J. H., Bernard, K. S., Daly, E. A., Zeman, S., Fisher, J. L., Brodeur, R. D. and Hurst, T. P. (2020) Implications of *Pyrosoma atlanticum* range expansion on phytoplankton standing stocks in the northern California Current. *Prog. Oceanogr.*, **188**, 102424.

Paffenhöfer, G. A., Stewart, T. B., Youngbluth, M. J. and Bailey, T. G. (1991) High-resolution vertical profiles of pelagic tunicates. *J. Plankton Res.*, **13**, 971–981.

Perissinotto, R., Mayzaud, P., Nichols, P. D. and Labat, J. P. (2007) Grazing by *Pyrosoma atlanticum* (Tunicata, Thaliacea) in the South Indian Ocean. *Mar. Ecol. Prog. Ser.*, **330**, 1–11.

Pomeroy, L. *et al.* (2007) *The microbial loop*, *Oceanogr. Soc.*, **20**, 28–33.

Purcell, J. E. and Madin, L. P. (1991) Diel patterns of migration, feeding, and spawning by salps in the subarctic Pacific. *Mar. Ecol. Prog. Ser.*, **73**, 211–217.

Sameoto, D. D. (1986) Influence of the biological and physical environment on the vertical distribution of mesozooplankton and micronekton in the eastern tropical Pacific. *Mar. Biol.*, **93**, 263–279.

Sato, M., Dower, J. F., Kunze, E. and Dewey, R. (2013) Second-order seasonal variability in diel vertical migration timing of euphausiids in a coastal inlet. *Mar. Ecol. Prog. Ser.*, **480**, 39–56.

Schram, J., Sorensen, H. L., Brodeur, R. D., Galloway, A. W. E. and Sutherland, K. R. (2020) Abundance, distribution, and feeding ecology of *Pyrosoma atlanticum* in the northern California Current. *Mar. Ecol. Prog. Ser.*, **651**, 97–110.

Silguero, J. M. B. and Robison, B. H. (2000) Seasonal abundance and vertical distribution of mesopelagic calycophoran siphonophores in Monterey Bay, CA. *J. Plankton Res.*, **22**, 1139–1153.

Steinberg, D. K., van Mooy, B. A. S., Buesseler, K. O., Boyd, P. W., Kobari, T. and Karl, D. M. (2008) Bacterial vs. zooplankton control of sinking particle flux in the ocean's twilight zone. *Limnol. Oceanogr.*, **53**, 1327–1338.

Stenvers, V. I., Hauss, H., Osborn, K. J., Neitzel, P., Merten, V., Scheer, S., Robison, B. H., Freitas, R. *et al.* (2021) Distribution, associations and role in the biological carbon pump of *Pyrosoma atlanticum* (Tunicata, Thaliacea) off Cabo Verde, NE Atlantic. *Sci. Rep.*, **11**, 9231.

Sutherland, K. R., Sorensen H. L., Blondheim O. N., Brodeur R. D., Galloway A. W. E. (2018) Range expansion of tropical pyrosomes in the Northeast Pacific Ocean. *Ecology* **99** 10 2397 2399

Thompson, A. W., Ward, A. C., Sweeney, C. P. and Sutherland, K. R. (2021) Host-specific symbioses and the microbial prey of a pelagic tunicate (*Pyrosoma atlanticum*). *ISME Commun.*, **1**, 11.

Townsend, D. W., Cucci T. L., Berman T. (1984) Subsurface chlorophyll maxima and vertical distribution of zooplankton in the Gulf of Maine. *J. Plankton Res.*, **6**, 793–802 5.

Van Soest, R. W. M. (1981) A monograph of the order Pyrosomatida (Tunicata, Thaliacea). *J. Plankton Res.*, **3**, 603–631.

Wiebe, P. H. *et al.* (2014) A vocabulary for the configuration of net tows for collecting plankton and micronekton. *J. Plankton Res.*, **37**, 21–27.